ROYAL SOCIETY OF CHEMISTRY

PAPER

Check for updates

View Article Online
View Journal | View Issue

Citric acid cross-linked honey and aloe vera gel loaded chitosan hydrogels for wound dressing applications

Sohail Shahzad,*[a] Ghulam Ghouse,[a] Muhammad Zubair, [b] Asma Yaqoob,[c] Maria Mujahid, [a] Faiz Ahmed, [d] Zahid Rauf[e] and Aman Ullah [b]*

Chronic wounds pose a global challenge, often requiring the use of multifunctional materials that facilitate healing while protecting against infection. The present study develops porous, biodegradable and antibacterial composite hydrogels from chitosan and polyvinyl alcohol (PVA) incorporating honey and aloe vera gel as antimicrobial agents for healing chronic wounds. Hydrogels were prepared by freeze gelation methodology, and further crosslinked with citric acid. FTIR spectra confirmed the presence of characteristic functional groups and showed a reduction in the peak intensities of O–H, N–H, and amide bands in crosslinked hydrogels. Scanning electron micrographs illustrated the clear morphological changes; citric acid crosslinked hydrogels (GG-05, GG-06, GG-08) exhibited more porous, sponge-like structures, with GG-08 achieving the highest porosity, having an average pore size of 21.28 µm. The hydrogel GG-08 demonstrated the greatest water retention capacity, reaching up to 218%, while GG-04 showed the highest degradation of 93% $\pm$ 3. The developed hydrogels exhibited better antibacterial properties, especially GG-03, GG-04, GG-07 and GG-08 had excellent activity against Gram-positive *Staphylococcus aureus* (*S. aureus*). Similarly, GG-01 and GG-05 showed excellent activities against Gram-negative bacterial strains, *i.e. Escherichia coli* (*E. coli*) and *Klebsiella pneumonia* (*K. pneumonia*). Anti-hemolytic testing confirmed the biocompatibility and non-toxic nature of hydrogels. The results demonstrated that citric acid addition has significantly improved the antibacterial potential against *E. coli* and *K. pneumonia* and also enhanced solution absorption, water retention and moisture content. Overall, these hydrogels demonstrated potential as advanced wound dressings, owing to their better moisture retention, broad-spectrum antibacterial properties and excellent biocompatibility.

1 Introduction

Hydrogels are extensively utilized as ideal wound dressing materials due to their remarkable ability to sustain moisture and facilitate the healing process.[1,2] Most importantly, they can absorb the wound exudates without the loss of nutrients.[3] Their three-dimensional network resembles extracellular matrix (ECM), thereby supporting cell adhesion and proliferation.[4,5] Compared to homopolymeric hydrogels, composite hydrogels offer improved strength, better water retention and other physico-chemical properties.[6,7] Natural biopolymers, including polysaccharides, proteins and synthetic polymers, have been used as hydrogels to accelerate wound healing in biomedical applications.[8–10]

Among these, chitosan, derived from crustacean exoskeletons, offers innate antibacterial activity and excellent biocompatibility,[11,12] with hemostatic and antioxidant properties.[13,14] However, its low mechanical strength can be enhanced by combining with PVA,[15] which develops double network hydrogels.[16] Chitosan/PVA[17] hydrogels are a preferable choice for wound dressings because they provide a stable and moist healing environment by combining the mechanical strength, flexibility, and hydrophilicity of PVA with the biocompatibility, biodegradability, and antibacterial qualities of chitosan. While alginate, hyaluronic acid, or polyethylene glycol hydrogels may offer enhanced absorption, regeneration, or durability, the chitosan/PVA blend presents an optimum equilibrium between antibacterial efficacy and structural integrity, particularly advantageous for wound care applications.[12]

Honey has been used for millennia as a traditional wound treatment. About 40% of honey is fructose, 10% is maltose, and 30% is glucose. Oligosaccharides, carbohydrates, minerals, enzymes, and phytochemicals make up honey.[18] Honey

[a] Department of Chemistry, University of Sahiwal, Sahiwal 57000, Pakistan. E-mail: drsohail@uosahiwal.edu.pk

[b] Lipids/Materials Chemistry Group (LMCG), Department of Agricultural, Food and Nutritional Science (AFNS), University of Alberta, Edmonton, AB, T6G 2P5, Canada. E-mail: ullah2@ualberta.ca

[c] Institute of Biochemistry, Biotechnology and Bioinformatics, The Islamia University of Bahawalpur, Pakistan

[d] Department of Chemistry, Government College University Faisalabad, Faisalabad 37000, Pakistan

[e] Pakistan Forest Institute (PFI), Peshawar, Khyber Pakhtunkhwa 25130, Pakistan

improves granulation and epithelization, eliminates infection, reduces inflammation, edema, and discomfort, regulates odor, and promotes healing with less scarring.[19] Its antimicrobial properties stem from high osmolarity, pH, H_2O_2 generation and phytochemicals. Sugar's osmotic effect prevents bacterial growth by removing water from cells, while maintaining moisture for wound healing.[20] Honey lowers wound pH, promotes fibroblast growth and angiogenesis, increases oxygen release from hemoglobin, and accelerates healing.[21] However, direct application of honey to wounds is difficult as it leaks out. Therefore, incorporating honey into a hydrogel system is more beneficial.[22] Similarly, Aloe vera is the most potent and commercially significant plant in aloe research.[23] About 200 active chemicals, including amino acids, carbohydrates, enzymes, vitamins, minerals, and salicylic acid are present, along with about 75 nutrients.[24] Aloe vera is known for its anti-aging, anti-inflammatory, antidiabetic, sunburn-treatment, and anticancer properties.[25] It stimulates cell growth and promotes skin regeneration, preventing scar formation after injuries.[26]

Freeze gelation represents an optimal and environmentally benign approach for the fabrication of these composite hydrogels.[27] Chemical crosslinking is often necessary to enhance the mechanical characteristics of hydrogels. The citric acid (CA), being an inexpensive, non-toxic and abundantly available chemical, is widely employed for crosslinking of polymer chains.[28] The hydroxyl groups (OH) and amino groups (NH$_2$) of polysaccharides and the carboxyl group (COOH) of CA have been shown to undergo physical or chemical interactions. The crosslinks are produced when one CA molecule combines with hydroxyl groups or amino groups from distinct polysaccharide chains. Furthermore, Gram-negative bacteria are also susceptible to the antibacterial action of residual amounts of CA cross-linker,[29] effective for sterilizing. It is well recognized that bacterial infections are a major cause of chronicity, which delays the healing of wounds since the bacteria may readily induce a persistent inflammatory response.[30]

This study combines chitosan/PVA hydrogels crosslinked with citric acid and natural bioactive ingredients (aloe vera gel and honey, Fig. 1) to prepare a multifunctional wound dressing with improved absorption, antimicrobial, and biocompatibility attributes. While chitosan/PVA hydrogels have been reported so far, mostly use hazardous synthetic crosslinkers like glutaraldehyde, limiting their use in the biomedical field. This work uses citric acid, a food-grade and biocompatible crosslinker, that enhances mechanical stability, water absorption, and porosity of hydrogels. The addition of honey and aloe vera improves swelling and water retention while altering internal microstructure and imparting natural antibacterial, anti-inflammatory, and wound healing properties. In addition, comparison of uncrosslinked and crosslinked formulations provides insights into how composition and morphology impact absorption behavior often not studied.

2   Materials and methods

2.1   Materials and reagents

The shrimp shell-derived chitosan, which has a molecular weight b/w 190–375 kDa, viscosity of 100–200 mpa s and a greater than
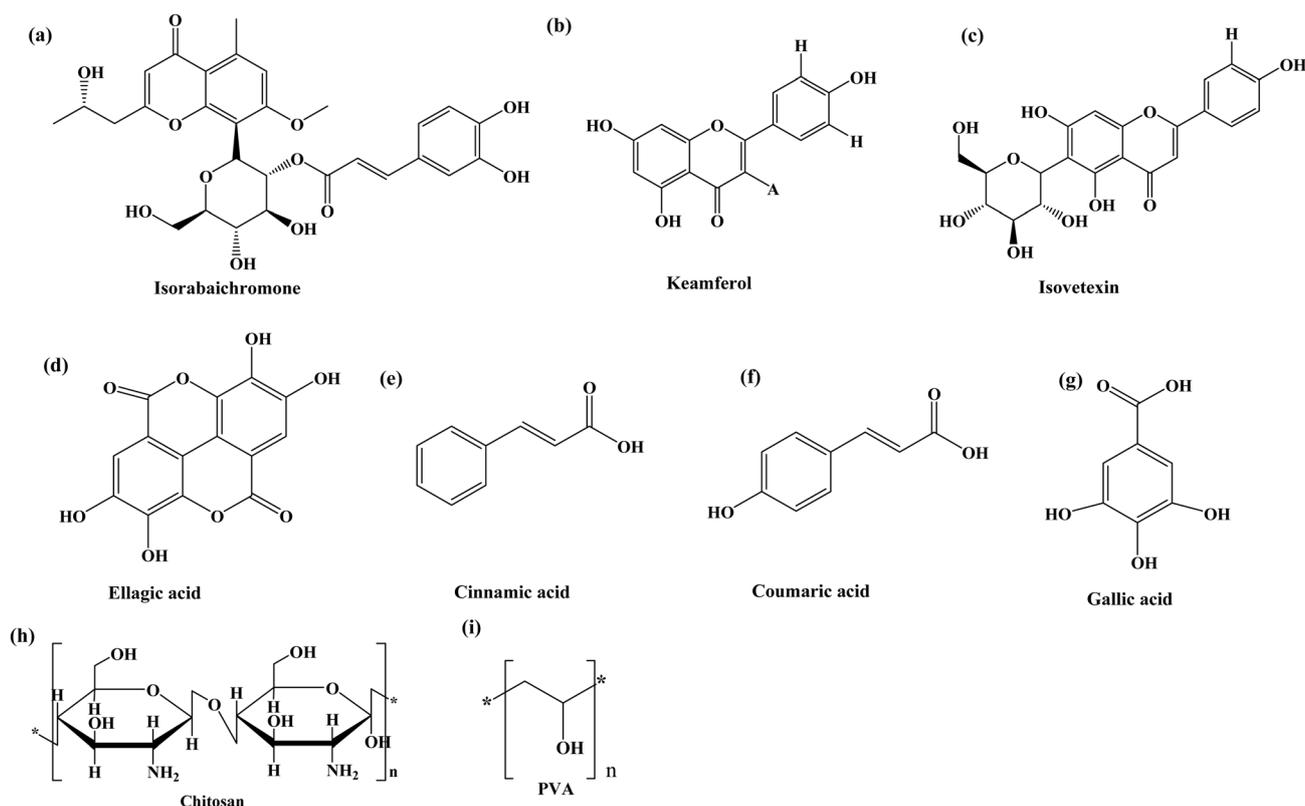

Fig. 1   Active components of aloe vera (a–c), honey (d–g), chitosan (h), PVA (i).

     © 2025 The Author(s). Published by the Royal Society of Chemistry

95% degree of deacetylation degree. Chitosan and citric acids were supplied by Macklin Chemicals (China). Glacial acetic acid was obtained from Chem-Lab (Belgium). PVA (degree of hydrolysis 98% and Mw: 72 000) was bought from Merck. Fresh aloe vera gel (AV gel) was extracted from an aloe vera plant in Sahiwal, Pakistan. Honey was bought from Marhaba Industries Pakistan. All tests were performed with deionized water. Pathogenic bacteria were taken from the bacterial bank of the Islamia University of Bahawalpur and activities were performed in its Institute of Biochemistry, Biotechnology and Bioinformatics. While blood sample was taken from blood bank of Bahawal Victoria Hospital (BVH), Bahawalpur-Pakistan. Analytical-grade solvents alongside chemicals were used as supplied by companies.

2.2 Preparation of crosslinked chitosan/PVA hydrogels loaded with aloe vera gel and honey

1 g of chitosan was dissolved in a 1% acetic acid solution and agitated for 4 hours at room temperature at 600 rpm to make a 1% (w/v) chitosan solution. A 5% (w/v) PVA solution was prepared by dissolving 5 g of PVA in the corresponding volume of deionized water. This was done at 90 °C while stirring continuously for 6 hours using a reflux condenser. Then various volume ratios of chitosan, PVA, aloe vera gel and honey (mentioned in Table 1) were mixed and blended vigorously for 6 hours at ambient temperature to get their homogeneous solutions. For the preparation of crosslinked hydrogels, 3 mL of 5% citric acid was additionally added to each solution. Then all the solutions were carefully transferred to eight Petri dishes. All Petri dishes were then kept in a freezer at −20 °C for 24 hours. Meanwhile, a 3 M ethanolic NaOH solution was prepared and subsequently cooled to a temperature of −20 °C. After 24 hours, an ethanolic NaOH solution was poured on each Petri dish, followed by keeping all Petri dishes again in the freezer for 48 hours at a temperature of −20 °C. After 48 hours, all hydrogels were placed at room temperature for 24 hours and then removed from Petri dishes and washed three times with approximately 10 mL of aqueous ethanol solution (50%), followed by washing with distilled water until a pH of 7.0 was obtained. The hydrogels were finally washed with pure ethanol and then dried at 37 °C. Hydrogels were coded as GG-01 to GG-04 (uncrosslinked) and GG-05 to GG-08 (crosslinked) (Fig. 2).

2.3 Characterization of synthesized hydrogels

2.3.1 FTIR spectroscopy.
Hydrogels' FTIR spectra were examined using a Thermo-Nicolet 6700 FTIR Spectrometer (USA). A photoacoustic method was used to take FTIR, with a frequency range of 4000–400 cm^{-1} and 256 consecutive shots at an accuracy of 8 cm^{-1}.

2.3.2 Morphological analysis.
Hydrogels comprehensive morphology was analyzed at different magnifications by SEM (model EmCrafts Cube II table top, South Korea). A 5 kV acceleration voltage was used to run the SEM. Before being observed, a small layer of gold was sputter-coated onto the freeze-dried hydrogels.

2.3.3 X-ray diffraction (XRD) analysis.
An EmCraft (South Korea) Bruker D8 ADVANCE diffractometer fitted with a Cube 10 sample holder was used for the X-ray diffraction (XRD) investigation. The system uses Cu Kα radiation ($\lambda = 1.5406$ Å) and operates in a θ–2θ configuration. It features a high-precision goniometer and LYNXEYE detector for accurate phase identification and structural analysis. The Cube 10 module supports automated sample handling for efficient and reproducible measurements.

2.3.4 Thickness of hydrogels.
A digital screw gauge micrometer (Insize, USA) with a 0–25 mm range was used to measure the thickness of the hydrogels in millimeters (mm). After taking five measurements of the hydrogel's interface, the arithmetic mean was determined.

2.3.5 Camera images.
Camera images were recorded for observation of hydrogels color, appearance and their homogeneous/uniform nature. The images were recorded using a mobile camera (vivo Y-200) with 64 megapixels.

2.4 Water retention capacity

First of all, fabricated hydrogels were cut into 20 × 20 mm^2 horizontally. These cut parts were weighed and submerged in deionized water and permitted to expand to attain stability. After wiping off extra water, the specimens were placed at room temperature for a day to get them dry, and then their weight was measured. Water retention was measured using the equation mentioned below.

$$\% \text{ Water retention capacity} = \frac{W_t}{W_0} \times 100 \quad (1)$$

Here, W_0 is the initial weight of hydrogel and W_t is the weight of swell hydrogel and dried gel after 24 hours.

Table 1 Chitosan, PVA, aloe vera gel, honey, and citric acid in different proportions by volume

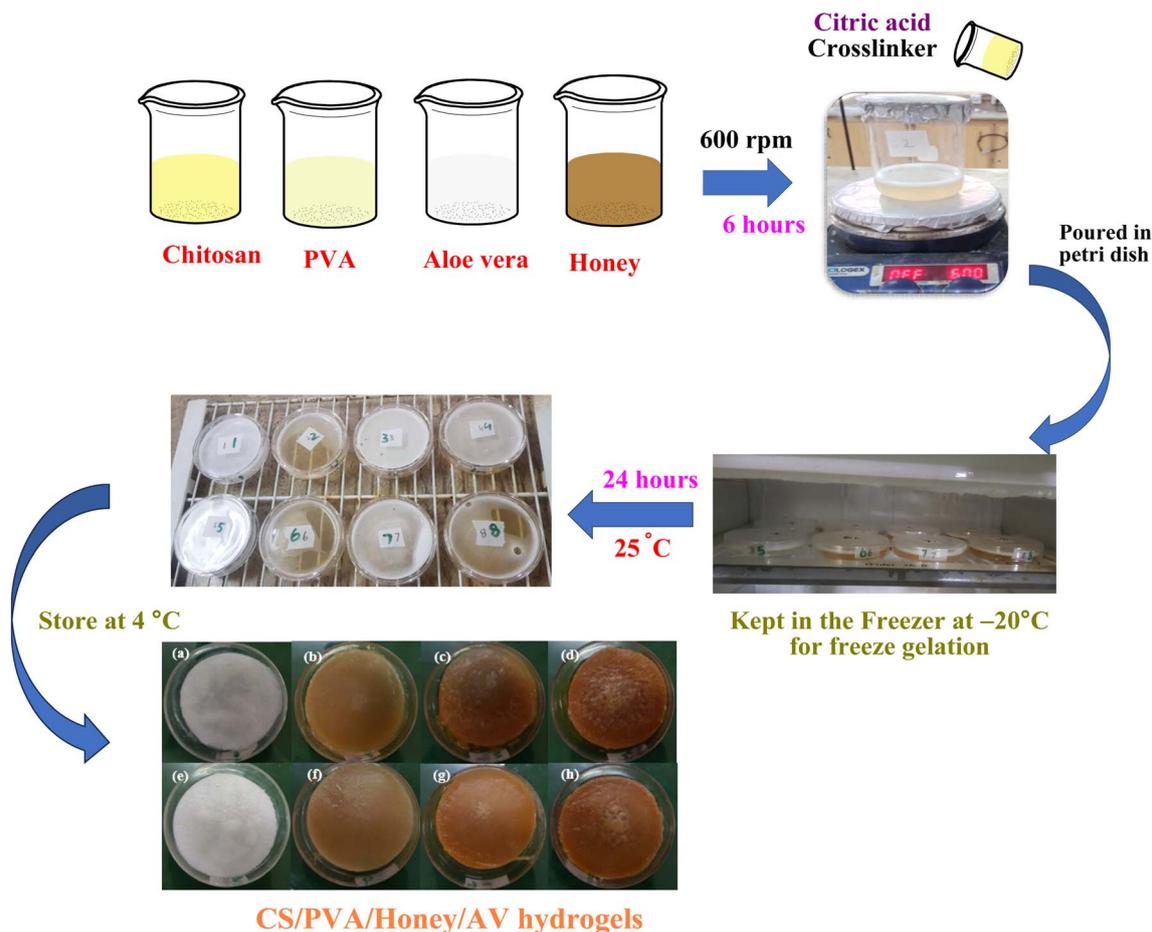| S. no.	Hydrogel code	Chitosan (mL)	PVA (mL)	Honey (mL)	Aloe vera gel (mL)	Citric acid (mL)
1	GG-01	20	20	—	—	—
2	GG-02	20	20	3	—	—
3	GG-03	20	20	3	3	—
4	GG-04	20	20	4	4	—
5	GG-05	20	20	—	—	3
6	GG-06	20	20	3	—	3
7	GG-07	20	20	3	3	3
8	GG-08	20	20	4	4	3

Fig. 2 Schematic diagram of fabrication of CS/PVA/aloe vera/honey based uncrosslinked and citric acid crosslinked hydrogels.

2.5 Moisture content

The percentage of moisture content (MC%) was calculated using the drying methodology's loss.[31] Hydrogels in tiny pieces were cut and weighed. After that, the synthesized hydrogels were placed in an oven set at 105 °C to completely dry out the fluid and achieve a consistent weight. MC% of hydrogels was measured using eqn (1).

$$\% \text{ Moisture content(MC)} = \frac{M_\mathrm{w} - M_\mathrm{d}}{M_\mathrm{w}} \times 100 \qquad (2)$$

where M_w and M_d represent the initial and dry hydrogel weights, respectively. This experiment was performed in triplicate, and average values were taken for calculations.

2.6 Solution absorption studies

PBS (phosphate buffered saline) solution with a pH of 7.4 was used to investigate the solution absorption capacity of all synthesized GG-01 to GG-08 hydrogels. Each hydrogel piece dried weight was calculated after it was cut into tiny bits. After that, the hydrogels were individually dipped in PBS solution, taken out every ten minutes, and their weight was recorded until the solution was fully absorbed. We used eqn (2) to compute the percentage of solution absorption.

$$\% \text{ Solution absorption(S)} = \frac{M_\mathrm{S} - M_\mathrm{d}}{M_\mathrm{d}} \times 100 \qquad (3)$$

Here, M_s denotes swollen weight and M_d denotes dried weight.

2.7 Antibacterial potential of hydrogels

Antibacterial behavior of all the fabricated hydrogels was assessed against *Staphylococcus aureus* (Gram-positive bacteria), *Escherichia coli* and *Klebsiella pneumonia* (Gram-negative bacteria) using the disc diffusion technique. In nutritional broth (Oxoid, UK), three distinct bacterial strains were grown for eight hours at 37 °C with 100 μL of suspension. After using sterile swabs to evenly distribute the bacterial culture on agar plates, the plates were allowed to dry for 20 minutes. After this, the hydrogels pieces were kept on agar plates. Each Petri plate covers a maximum of three sample discs placed approximately at equal distance to one another. Positive control was prepared from a standard commercial antibiotic drug having a concentration of 10 μg mL^{-1} of ciprofloxacin for all three bacterial strains. Finally, the agar plates were preserved at 4 °C for two hours and then incubated for 18 to 24 hours (depending upon the type of bacteria) at 37 °C, and were observed for an inhibition zone, which is measured by calipers. Antibacterial ability of hydrogels was evaluated by calculating the inhibition zone

diameter in millimeters (mm) and by making a comparison with the positive control.[32]

2.8 Biodegradation analysis

Analysis of hydrogel biodegradation was conducted in a PBS solution at pH 7.4. After being cut and weighed (W_1), small pieces of hydrogel were immersed in PBS solution for 42 days at 37 °C. After 42 days, gels were removed, wiped out and dried at 37 °C for 24 hours and then weighed (W_2) again. The % weight loss of all hydrogels was calculated using eqn (3).

$$\% \text{ Weight loss} = \left[\frac{W_2}{W_1}\right] \times 100 \tag{4}$$

2.9 Anti-hemolytic/cytotoxicity analysis

Hemolytic analysis of hydrogels was performed by previously reported method.[33] 3 mL of fresh heparinized bovine blood were obtained and centrifuged at 1000 rpm for ten minutes. The plasma was disposed of and leftover red blood cells (RBCs) were rinsed 3 times using a chilled (4 °C) aseptic PBS solution having a pH value of 7.4. RBCs were maintained at 10^8 cells per milliliter for every test. 20 μL sample solutions (released from hydrogels) were taken and mixed with RBCs, individually after pre-weighed hydrogels (10 mg) were soaked in 1 mL of distilled water. After 45 minutes of incubation at 37 °C, all hydrogel samples were shaken for ten minutes. Following five to ten minutes on ice, the hydrogel samples were centrifuged once more for ten minutes at 1000 rpm. After extracting 100 μL of supernatant from each tube, it was diluted ten times using a cooled (4 °C) PBS (pH 7.4) solution. Negative control was PBS (pH 7.4) solution, while Triton X-100 (0.1% v/v) was taken as positive control. Finally, absorbance was measured at 576 nm with a UV spectrophotometer. Breakdown of RBCs percentages by each hydrogel and control were computed.

3 Results and discussions

3.1 Structural, morphological and visual analysis

FTIR was run to confirm the presence of different active functional groups of individual constituents of hydrogels, including chitosan, PVA, aloe vera gel, honey and citric acid. It was also used to evaluate certain interactions and crosslinking between chitosan and PVA chains within the hydrogels, in the presence of citric acid, which was being used as a crosslinking agent. FTIR spectra of uncrosslinked hydrogels GG-01, GG-02 and GG-03 and crosslinked hydrogels GG-05, GG-06 and GG-07 are presented in Fig. 3. FTIR spectra in Fig. 3 showed that all individual spectrums of hydrogels are exhibiting some common peaks at the same wavenumber. This was due to their similar composition of chitosan and PVA. In addition to this, FTIR individual spectrums of hydrogels also exhibited certain variations in terms of changes in peaks intensities and width due to the incorporation of aloe vera gel, honey and citric acid. Some common peaks exhibited by all spectra in Fig. 3 were the presence of a wide peak from 3500–3100 cm^{-1} (O–H and N–H stretching vibrations),[34,35] and a relatively sharp and minor peak at 2890–2870 cm^{-1} (alkyl C–H stretching vibration).[31] Similarly, certain other common peaks appeared at 1650 cm^{-1} (amide-I), 1530 cm^{-1} (amide-II), 1380 cm^{-1} (O–H bending) and 1060 cm^{-1} (C–O–C stretching).[36] When we compared spectrum GG-01 (having only chitosan and PVA) and GG-05 (having chitosan, PVA and citric acid), it was observed that certain peaks intensity and values were slightly changed, as evident from Fig. 3. It was observed that N–H and O–H stretching vibrations peak (3500–3100 cm^{-1}) intensity was slightly decreased, due to participation of these groups in making interactions with citric acid and constructing crosslinking. Similarly slight decrease in intensity of the amide-I band was observed at 1650 cm^{-1}, which also indicated the development of certain new interactions among functional groups of chitosan and PVA within this spectral range. Spectrum GG-02 (having chitosan, PVA and honey) and
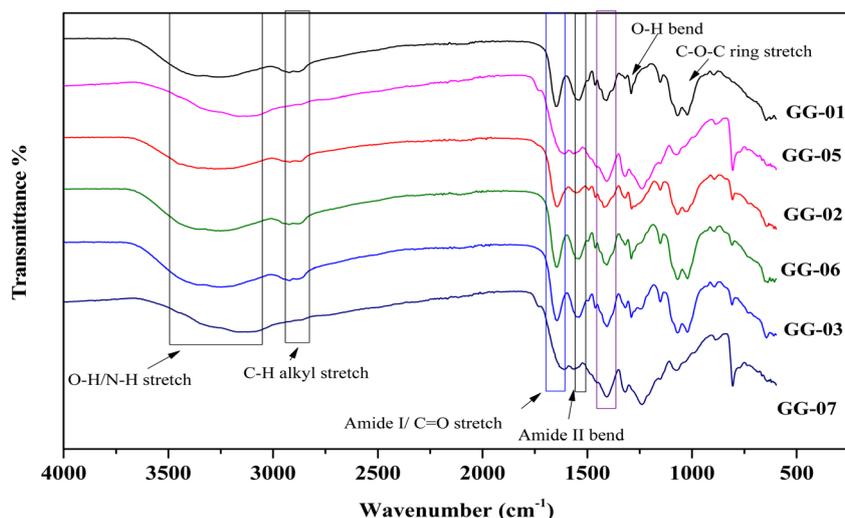

Fig. 3 FTIR spectra of hydrogels GG-01, GG-02 and GG-03 (uncrosslinked) and GG-05, GG-06 and GG-07 hydrogels (crosslinked).
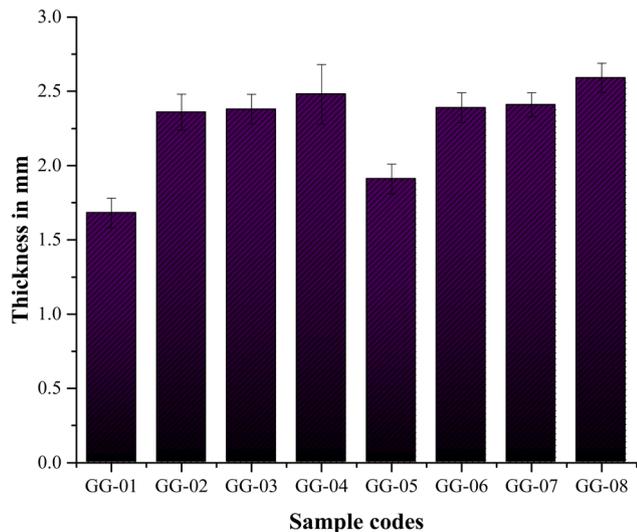
Fig. 4 Thickness of synthesized hydrogels in mm.

spectrum GG-06 (having chitosan, PVA, honey and citric acid) have also shown a significant decrease in N–H and OH stretching vibrations and a decrease in intensities of amide-I and amide-II band peaks. This further supported that the crosslinking phenomenon has occurred. In the same way, spectrum GG-03 (having chitosan, PVA, honey and AV gel) and spectrum GG-07 (having chitosan, PVA, honey, AV gel and citric acid) have displayed substantial decline in N–H and OH stretching frequencies and amide-I and amide-II peaks intensities. Thus, FTIR confirmed that citric acid played a very crucial role in imparting crosslinking to polymer chains and provided strength to the hydrogels.

Hydrogels thickness values were measured in the range of 1.68 mm (GG-01) to 2.59 mm (GG-08) and the values are presented in graphical form in Fig. 4 and were also mentioned in Table 2. The results showed that gradually increasing the volume ratios of chitosan, PVA, honey, aloe vera gel and citric acid has increased the thickness of gels. GG-01 and GG-05 hydrogels were found to be thin due to the absence of honey and aloe vera gel. The addition of 3 mL honey into GG-02 and GG-06 enhanced their thickness. Moreover, the addition of 3 mL of aloe vera gel (in addition to honey) into GG-03 and GG-07 further increased thickness. Finally, the incorporation of

4 mL of honey and aloe vera gel has further improved their thickness.

Visual appearance including color, texture and homogenous nature of hydrogels were observed with camera images presented in Fig. 5. Fig. 5(a–d) represent the uncrosslinked hydrogels (GG-01 to GG-04) while Fig. 5(e–h) represent crosslinked hydrogels (GG-05 to GG-08). The camera images of GG-01 and GG-05 showed their off-white color and homogeneous nature. These hydrogels contain only chitosan and PVA in their composition. Hydrogels GG-02 and GG-06 (incorporating chitosan, PVA and honey) appeared to be yellowish brown in color and were observed to be completely homogenous. Similarly, hydrogels GG-03, GG-04, GG-07 and GG-08 (incorporating chitosan, PVA, honey and aloe vera gel) were completely uniform and dark brown in color. It was inferred that the addition of honey has contributed majorly to the change of color from off-white transparent to yellowish or brownish, while aloe vera gel has also contributed partially. All the hydrogels were seen and observed as strong, smooth and homogeneous.

The hydrogel's network of interconnected pores enables effective permeability of gases and wound fluids, and facilitates attachment and proliferation of cells, and speeds up wound healing. The hydrogel's porosity is essential for promoting cell adhesion, growth, and extracellular matrix deposition.[37] Surface morphology of hydrogels was analyzed in a detailed manner using SEM. Fig. 6(a–c) (GG-01 hydrogel) showed highly fibrous morphology, due to chitosan and PVA strong intermolecular connectivity which mainly occurs through hydrogen bonding.[38] In comparison to the GG-01 hydrogel, Fig. 6(d–f) represents GG-02 hydrogel (having chitosan, PVA and honey), which displayed a smoother and spongy structure. This was due to honey's plasticizing action, which was demonstrated by the long, flexible strands that seemed to be present within the matrix, as honey makes the matrix more flexible and tends to make polymeric structures less rigid.[39] Fig. 6(g–i) represents GG-04 hydrogel (having chitosan, PVA, honey and aloe vera gel) and appeared to be more smoother, spongy and gel-like due to the presence of bioactive ingredients in aloe vera gel, particularly polysaccharides (acemannan), which reduces the stiffness in the hydrogel.[40] Aloe vera gel and honey both function as plasticizers and provide a more flexible nature to hydrogel and enhanced capacity for moisture retention, which is advantageous for wound dressings.[41]

Table 2 Physiochemical parameters of hydrogels

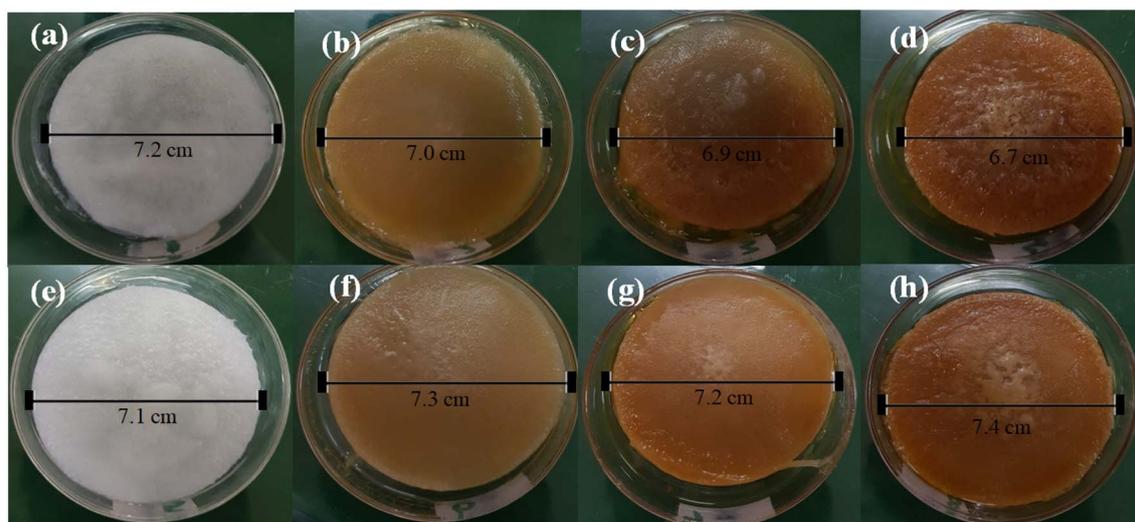| Sample code	Membrane thickness (mm)	% Water retention capacity	% Moisture content	% Degradation
GG-01	1.68 ± 0.04	150 ± 4	70 ± 2	67.8 ± 1.5
GG-02	2.36 ± 0.06	179 ± 5	84 ± 2	83.8 ± 2
GG-03	2.38 ± 0.03	198 ± 6	85 ± 2.5	86 ± 2
GG-04	2.48 ± 0.07	205 ± 8	93 ± 3	93 ± 3
GG-05	1.91 ± 0.04	180 ± 4	79 ± 2	54 ± 1
GG-06	2.39 ± 0.02	195 ± 4	87 ± 2	71 ± 2
GG-07	2.41 ± 0.05	211 ± 6	90 ± 3	76 ± 2.5
GG-08	2.59 ± 0.06	218 ± 4	99 ± 3.5	81 ± 3

Fig. 5 Camera images of (a) GG-01 (b) GG-02 (c) GG-03 (d) GG-04 (e) GG-05 (f) GG-06 (g) GG-07 (h) GG-08 hydrogels displaying the diameter on the scale bar.

Fig. 7(a to f) were used to represent citric acid crosslinked hydrogels (GG-05, GG-06 and GG-08) micrographs. Hydrogel GG-05 incorporated only chitosan, PVA and citric acid, while GG-06 contains chitosan, PVA, honey and citric acid, and GG-08 incorporates chitosan, PVA, honey, aloe vera gel and citric acid. It was inferred that these micrographs are clearly different from uncrosslinked hydrogel micrographs in Fig. 6(a to i). The hydrogel GG-05 in Fig. 7(a and b) showed irregular,
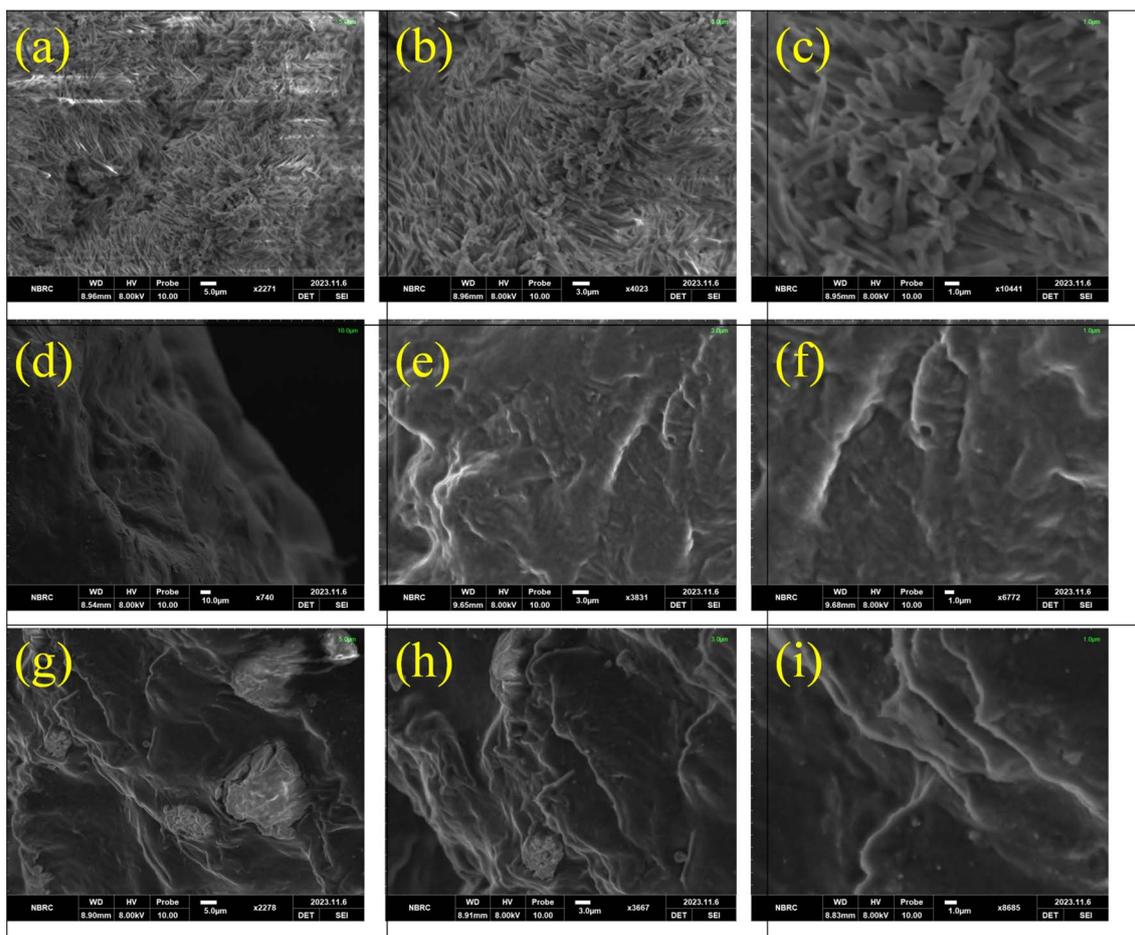

Fig. 6 SEM images of hydrogels GG-01 (a–c); GG-02 (d–f) and GG-04 (g–i) at different magnifications.
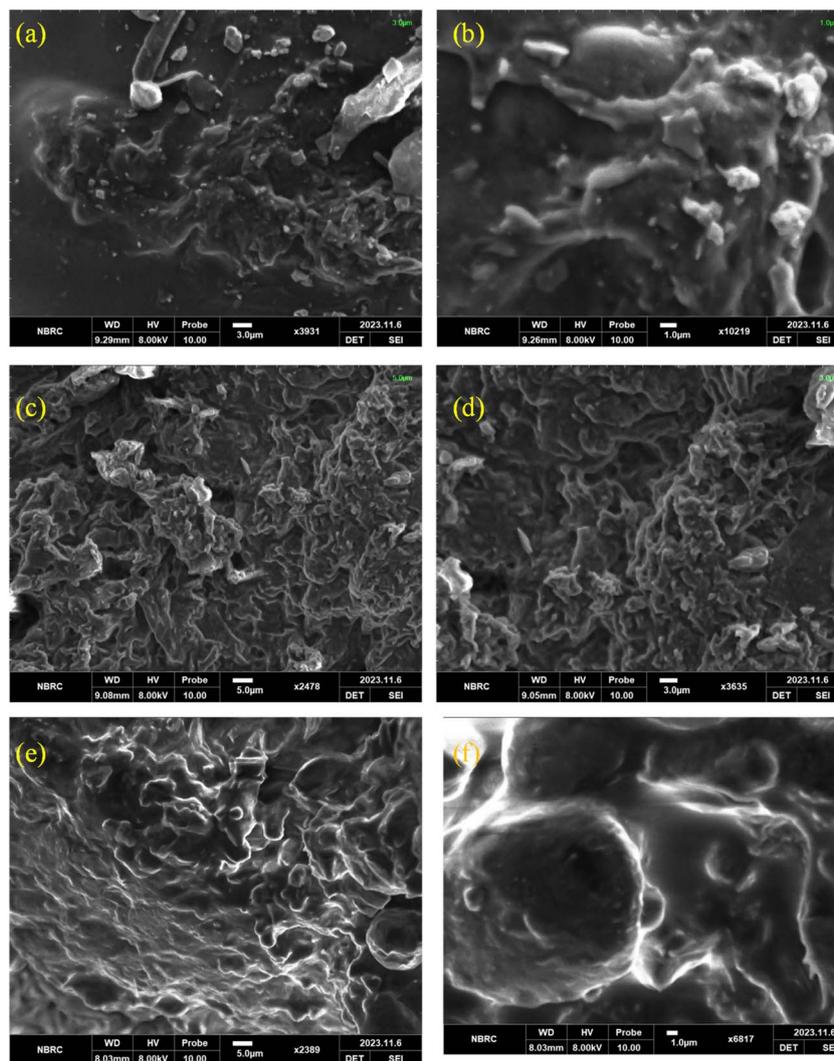
Fig. 7 SEM images of GG-05 (a and b); GG-06 (c and d) and GG-08 (e and f).

heterogeneous and a few white crystalline portions in its morphology because of citric acid's crosslinking effect, which strengthens the intermolecular interactions between chitosan and PVA with a smaller number of pores having a pore size of 22.34 μm. Similarly, micrographs in Fig. 7(c–f) for GG-06 have a pore size of 32.61 μm, and GG-08 hydrogels showed a highly sponge-like and porous structure, having a pore size of 21.28 μm. Thus, the SEM results clearly demonstrated that a more spongy and highly porous structure was created due to the introduction of citric acid as a crosslinking agent, especially in the presence of honey and aloe vera gel. This might be due to the creation of a large number of new intermolecular interactions between chitosan, PVA, honey, aloe vera gel and citric acid, which highly modified the morphology of hydrogels.[42]

3.2 XRD analysis

The synthesized hydrogels crystalline or amorphous nature was examined using XRD analysis. Fig. 8 showed the XRD graphs of the hydrogels that were developed, GG-01 hydrogel showed
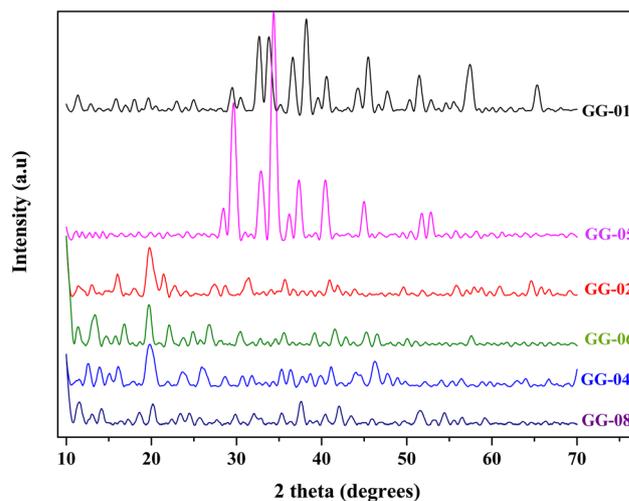

Fig. 8 XRD graph of uncrosslinked (GG-01, GG-02 and GG-04) and cross-linked (GG-05, GG-06 and GG-08) hydrogels.

© 2025 The Author(s). Published by the Royal Society of Chemistry

distinct and strong peaks, particularly in the 20–40° (2θ) range, which suggested its high crystallinity. While in GG-05 hydrogel, the polymer matrix becomes more flexible and amorphous as a result of citric acid reduction of crystallinity, as demonstrated by the XRD data.[43] The peaks in the GG-02 and GG-04 hydrogels are less intense which demonstrated that the addition of honey (in GG-02) and citric acid (in GG-06) has interacted with active functional groups of chitosan and PVA and thus produced profound effect by acting as plasticizer (honey) and crosslinker (citric acid) and induced amorphous phase to both of these hydrogels.[44]

Similarly, in GG-04 hydrogel, there are more amorphous regions and fewer crystalline regions as a result of disruption in the polymer chains' regular arrangement. The addition of honey and aloe vera gel introduces a variety of natural substances, including sugars from the honey and bioactive compounds of the aloe vera gel, which may disrupt the normal packing of the PVA and chitosan chains.[45] It is believed that increasing the volume of honey and aloe vera gel lowers their crystallinity. GG-08 hydrogel, more amorphous with less ordered, crystalline zones, which is reflected in the XRD pattern with broader and less intense peaks. The polymer matrix becomes more flexible and amorphous as a result of citric acid reduction of crystallinity, as demonstrated by the XRD data. In general, more amorphous materials are more malleable and appropriate for biomedical applications particularly for wound dressings.[46]

3.3 Water retention capacity (%)

Fig. 9 highlights the variations in the percent water retention capacity of various hydrogels from GG-01 to GG-08. The values of percent water retention capacity have also been mentioned in Table 2. The assay results exhibited that the lowest % water retention capacity (150%) was shown by GG-01, whose main composition was chitosan and PVA. The percent water retention capacity was increased in GG-02 hydrogel (179%), as it additionally contains honey in its composition, which is hydrophilic

due to its excessive sugar content. Further addition of aloe vera gel in GG-03 hydrogel further improved the percent water retention capacity of hydrogels to 198%, due to the moisturizing and water-holding properties of aloe vera gel. So, both honey and aloe vera gel improved hydrogel's capacity to absorb and retain water. The hydrogel GG-04, incorporating higher volume ratios of both honey and aloe vera gel further enhanced its ability to retain water up to 205%.[47]

GG-05, GG-06, GG-07, and GG-08 showed further improvements in % water retention capacities, due to the incorporation of citric acid, which is hydrophilic and contains hydroxyl and carboxyl groups in its structure, which make hydrogen bonds with water. Additionally, citric acid produced crosslinks between chitosan and PVA chains and promoted the formation of a more organized hydrogel network or improved hydrogel characteristics of the synthesized materials. The crosslinking has modified the internal structure of hydrogels and enhanced their porosity and giving hydrogels a spongy look, as evident from SEM images. Thus, GG-08 had shown the highest water retention capacity up to 218%, due to the presence of honey, aloe vera gel and citric acid addition to chitosan and PVA. Thus, GG-08 hydrogel indicated that this sample has the best balance between crosslinking strength and water absorption capacity since it contains the ideal ratios of citric acid, honey and aloe vera gel, and porous structure due to gelation. Overall, the graph showed that formulations with higher concentrations of hydrophilic additives, i.e. honey and aloe vera gel and citric acid, improved water retention, which made GG-08 the best option for applications that need constant moisture, like chronic wound care, where healing is aided by prolonged hydration.[48]

3.4 Moisture content (%)

The measurement of percent moisture content is a crucial parameter for hydrogels, and the results for both GG-01 to GG-
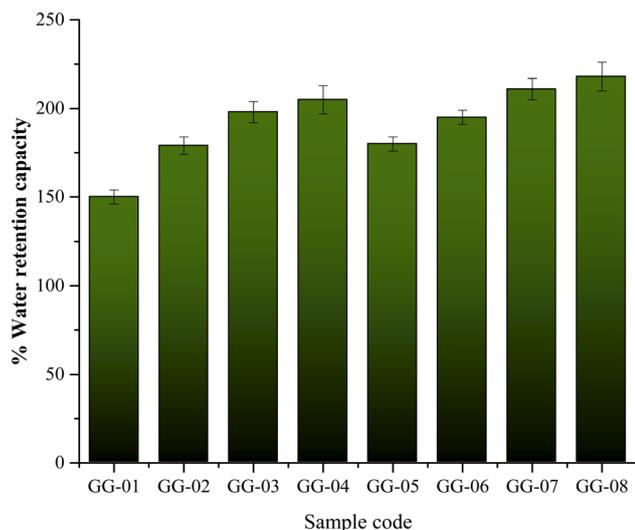

Fig. 9 Water retention capacity of all GG-01 to GG-08 synthesized hydrogels.
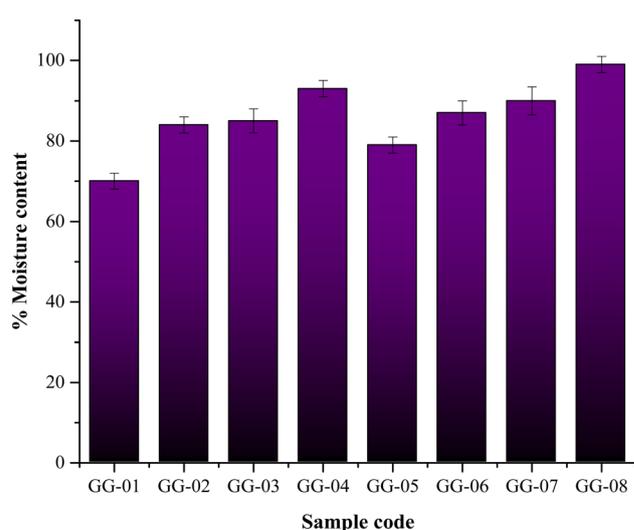

Fig. 10 Graph depicting the percentage of moisture content in the synthesized hydrogels.

04 (uncrosslinked) and GG-05 to GG-08 (cross-linked) hydrogels are shown in graphical form in Fig. 10 and their values are also mentioned in Table 2. The results demonstrated that hydrogel GG-01 exhibited lowest moisture content (70%) as depicted in Fig. 8. The hydrogel GG-01 was observed to be stiffer and less hydrophilic. The incorporation of honey in GG-02 hydrogel and both honey and aloe vera in GG-03 and GG-04 hydrogels further enhanced the moisture absorption capability of hydrogels, which clearly demonstrated the natural additives capacity to draw and hold water, because of their hydrophilic and moisturizing properties. Amongst uncrosslinked hydrogels, GG-04 had shown the maximum moisture content of 93%. Similar behavior and pattern of moisture absorption was observed in crosslinked hydrogels GG-05 to GG-08, where GG-08 has absorbed the maximum moisture content % of 99. The slight increase in absorption was attributed to the addition of citric acid in crosslinked hydrogels, which affected the morphology of crosslinked hydrogels and raised their ability to absorb and retain moisture. Thus, GG-08 could be a perfect material to be used for extended moisture absorption and thus used in dressings for chronic or extremely exudative wounds.[49,50]

3.5 Percent solution absorption studies of synthesized hydrogels

The absorption capacity of hydrogels is primarily controlled by hydrogen bonding and electrostatic interactions. These interactions occur between water molecules in the surrounding environment and hydrophilic functional groups such as –OH, –COOH, and –NH$_2$, leading to the expansion of the polymeric network.[51] While the absorption capacity of crosslinked hydrogels is controlled by the crosslinking density, pore size, network shape and osmotic pressure. Structure-related factors like surface area and charge density have a significant impact on the adsorption of solutes, which can also happen through hydrophobic interactions, electrostatic attraction, or specific functional group b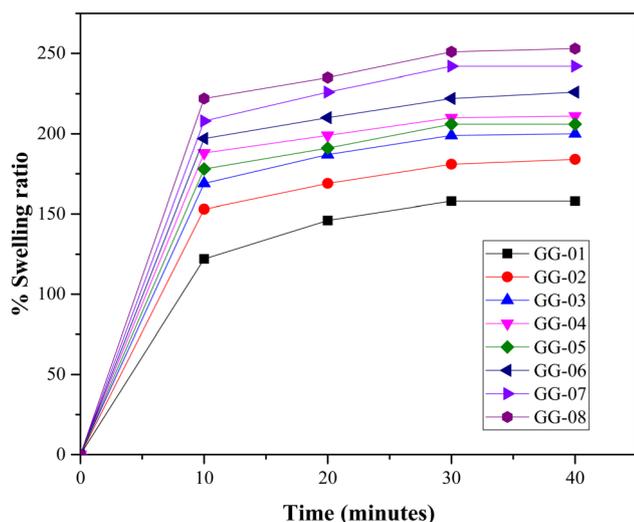inding.[35,52] Fig. 11 was used to explain the outcomes of the solution absorption analysis of each hydrogel in a PBS pH 7.4. It can be clearly seen from the graphs that hydrogels exhibited the highest level of solution absorption during the first 10 minutes, and within 30 to 40 minutes all hydrogels attained the equilibrium. The results revealed that both varying ratios of chitosan, PVA, honey, aloe vera gel and crosslinking with citric acid (which changed the morphology of hydrogels) had both impacted the ability of hydrogels to absorb and retain solution within their structure. Thus, solution absorption phenomenon was greatly affected by the functional groups that are present within hydrogel network. When compared the results of GG-01 (uncrosslinked) and GG-05 (crosslinked), the GG-01 hydrogel (which contains only CS and PVA) absorbed slightly less % of the solution due to the hydrophilic nature of PVA and chitosan's macromolecular chains, which contain ionizable functional groups –NH$_2$ and –OH, which aided in water accessibility.[31] While GG-05 showed better % solution absorption, due to citric acid ability to crosslink by creating physical linkages between its carboxyl groups and hydroxyl groups of PVA or chitosan, the crosslinked network became more hydrophilic and ultimately improved % solution absorption.[53] Similar behavior of % solution was observed in GG-02 (uncrosslinked) and GG-06 (crosslinked) hydrogels, but these hydrogels absorbed more solution % due to their additional honey component, as its nature is hydrophilic and it also greatly modified the internal structure of the hydrogel, especially of the GG-06 crosslinked hydrogel, as evident from SEM images.[54] Similarly, GG-03 and GG-07 hydrogels showed further improvement in absorption of solution due to the synergetic effects of both honey and aloe vera gel. Here, GG-07 absorbed more solution as compared to GG-03, due to its crosslinked and probably more sponge-like nature.[55] The results concluded that amongst uncrosslinked hydrogels, GG-04 showed maximum % solution absorption due to increased ratios of both honey and aloe vera gel. Similarly, GG-08 showed maximum solution absorption % amongst all hydrogels due to its crosslinked nature, which greatly altered and improved its morphology and made it a more porous and sponge-like structure as apparent from SEM images. This nature of hydrogel is most suitable for chronic wound care that requires a moist environment for extended periods.[56]

3.6 Antibacterial activities

The antibacterial properties of chitosan/PVA based hydrogels enriched with honey and aloe vera gel and further crosslinked with citric acid were tested against *S. aureus* (Gram-positive), *E. coli* (Gram-negative) and *K. pneumoniae* (Gram-negative). The antibacterial activity results were depicted in Fig. 12 in terms of inhibition zones and in graphical form in Fig. 13. The hydrogels' ability to effectively inhibit against above mentioned three bacterial strains is indicated by the inhibition zones. As a standard for the hydrogels' antibacterial effectiveness, the positive control sample (ciprofloxacin) exhibits maximum inhibition zone and the results were compared with the positive control. The antibacterial results showed that hydrogels different responses against different bacterial types. In case of *S. aureus*

Fig. 11 Results of % solution absorption tests for each hydrogel are shown graphically.

(a Gram-positive bacteria) hydrogels incorporating honey, aloe vera, and citric acid (GG-02, GG-3, GG-04, GG-6, GG-07 and GG-08) exhibited better to excellent activities. Hydrogel GG-02 showed comparatively better results against both *S. aureus* and *E. coli*, due to the addition of honey, which contributed to providing antibacterial activity due to the presence of high sugar contents (glucose and fructose), low water activity, acidic pH, and the presence of bioactive phenolic compounds, hydrogen peroxide and certain enzymes, which further enhanced its effectiveness. The result against *K. pneumoniae* was observed to be very weak. Similarly, GG-03 hydrogel exhibited slightly better antibacterial potential against all three selected bacterial strains, due to the presence of both honey and aloe vera gel. The antibacterial activities of GG-04 hydrogel were greatly enhanced especially against *S. aureus* and *K. pneumoniae*, due to an increase in volume ratios of both honey and aloe vera in these hydrogels. The GG-06 hydrogel, additionally incorporating honey, showed better antibacterial potential against all three selected strains. The GG-07 hydrogel, having both honey and aloe vera gel exhibited significant potential against both *S. aureus* and *K. pneumoniae*, while GG-08 exhibited superior effectiveness against *S. aureus* and *E. coli*, and while weakest potential against *K. pneumoniae*.

Likewise, GG-01 and GG-05 hydrogels showed excellent antibacterial potential against *E. coli* and *K. pneumoniae* (Gram-negative bacteria) due to the presence of chitosan in a higher ratio as compared to other hydrogels as other hydrogels were diluted due to the addition of honey and aloe vera. It is believed that the addition of citric acid has protonated the amino group of chitosan to produce a positive charge on its surface. Thus, by reacting with the negatively charged bacterial surface, it breaks
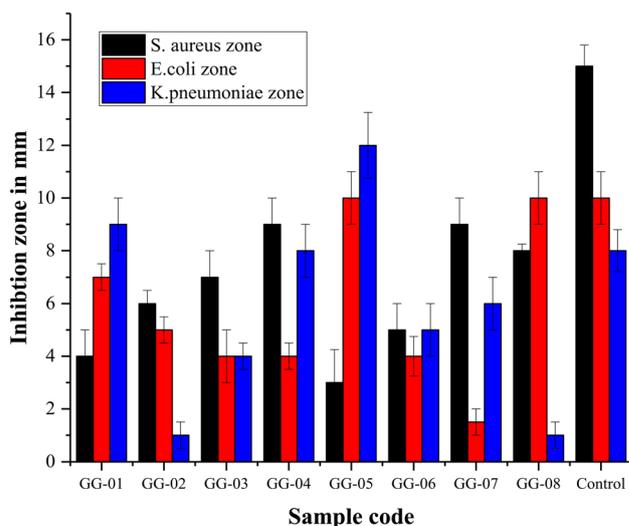

Fig. 13 Graphical illustration of antibacterial activities of hydrogels against *S. aureus*, *E. coli*, *K. pneumoniae* and compared with control (ciprofloxacin).

down the bacterial cell membrane, resulting in the leakage of intracellular contents leading to cell death.[57] Further, it is believed that crosslinking enhances stability and regulates chitosan release, thus providing better antibacterial potential.

Overall antibacterial potential was attributed to synergistic effects of chitosan, active phenolic compounds, sugars, hydrogen peroxide and enzymes in honey and various components including acemannan, vitamins, enzymes and anthraquinone present in aloe vera gel.
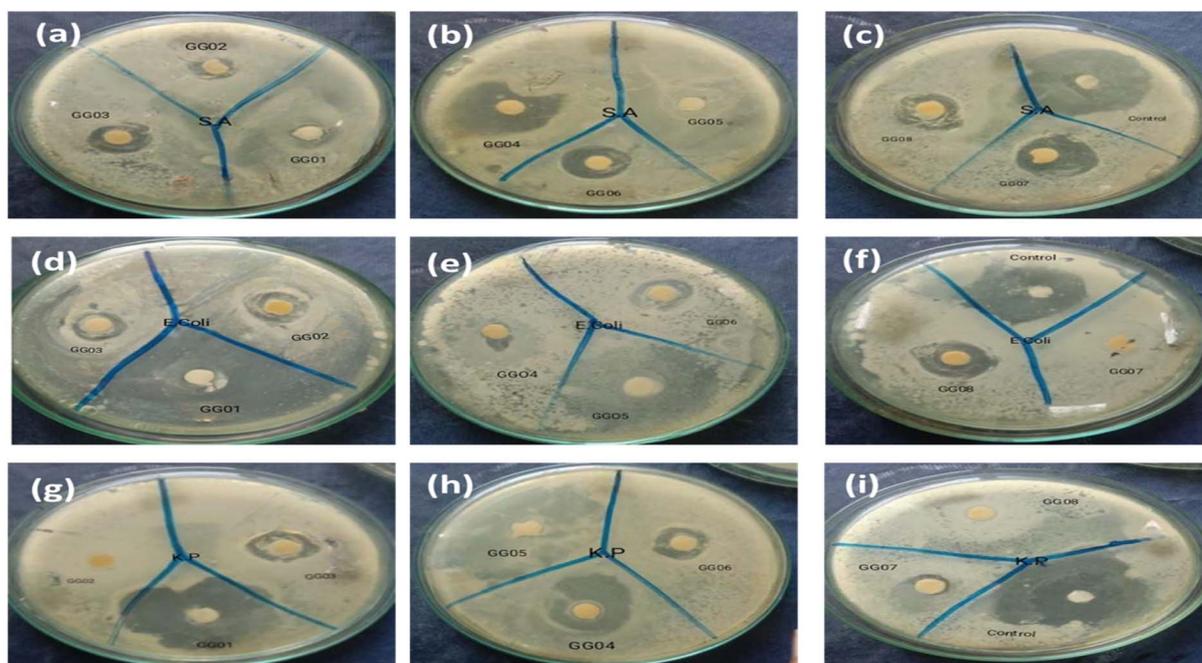

Fig. 12 Antibacterial activities of hydrogels against *S. aureus* (a–c), *E. coli* (d–f) and *K. pneumoniae* (g–i) compared with control (ciprofloxacin) in terms of inhibition zone.
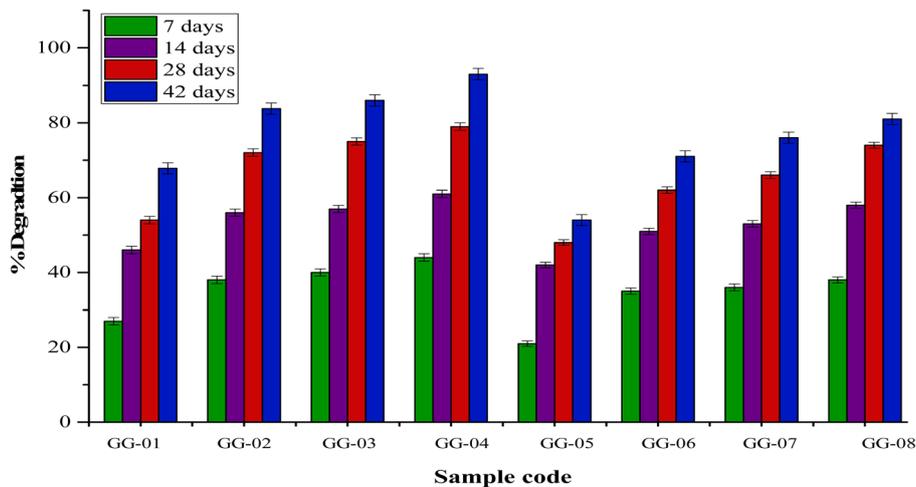
Fig. 14 Visual depiction of the biodegradation of synthetic hydrogel.

3.7 Biodegradation studies

The ability of biomaterials to biodegrade is essential for wound dressings because it promotes cell adhesion and proliferation, which improves wound healing and reduces scarring.[58] Gravimetric degradation experiments were conducted for each composition of the prepared hydrogel samples to assess the degradation rate. The hydrogels were stored in a solution of PBS at a temperature of 37 °C, spanning various time intervals ranging from day 1 to day 42. Table 2 provides the degradation values of hydrogels. The degradation rate of uncrosslinked hydrogels (GG-01, GG-02, GG-03 and GG-04) was found to be greater than crosslinked hydrogels (GG-05, GG-06, GG-07, GG-08). The slower degradation rate of crosslinked hydrogels was ascribed to their more complex and 3-dimensional (3D) interconnected network of polymer chains, which made it more difficult for water molecules to reach and break down the polymer chains.[59] The GG-01, made of chitosan and PVA exhibited 67.8% degradation after 42 days, while GG-05, having a similar composition of chitosan and PVA but crosslinked with citric acid, showed 54% degradation. Analogously, addition of honey in GG-02 (uncrosslinked) has shown enhanced % degradation of 83.8%, while GG-06 (crosslinked) exhibited 71% degradation, due to the hydrophilic nature and presence of water-soluble glucose and fructose sugars in honey.[60] Similarly, the degradation rate was further increased by the addition of aloe vera gel, as in GG-03 (86%) and GG-07 (76%). The natural polysaccharides (acemannan and glucomannan) and enzymes found in aloe vera gel, which acted as biodegradable fillers and interacted with chitosan/PVA based hydrogels framework.[10,61] The highest rate of degradation was expressed by GG-04, which is 93% because of high volumes of honey and aloe vera gel. Uncrosslinked hydrogels rehydrate dry wounds and thus provide moisture, which promotes tissue regeneration and speeds up the healing process.[62] While crosslinked hydrogels have the lowest degradation rates (Fig. 14), suitable for chronic wounds and burns, as well as for infected wounds, which require long-term care.

3.8 Anti-hemolytic analysis

Fig. 15 shows the hemolytic activity of the various hydrogel samples (GG-01 through GG-08) in comparison to the control. Since hemolytic activity indicates the hydrogel's capacity to lyse red blood cells, thus assessing cytotoxicity of a substance, *i.e.* ability of a chemical or substance to kill cells. It is thus a crucial biocompatibility indicator. The results of the assay indicated that GG-01 hydrogel exhibited the lowest hemolytic activity (2.71%), followed by GG-05 and GG-02. All synthesized hydrogels hemolytic values fall within acceptable bounds to be used in biomedical applications. Thus, hydrogels were proven to be non-toxic and biocompatible and can be used in wound healing applications without seriously harming red blood cells.[63] Hemolytic activity was noted to increase as honey, aloe vera gel and citric acid were added to the hydrogels. The highest hemolytic activity amongst all hydrogels was shown by GG-08 (11.43%). This slight increase in activity could be due to the
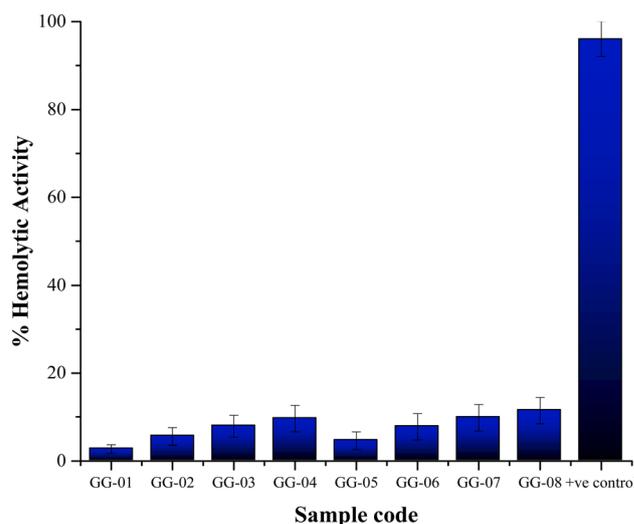

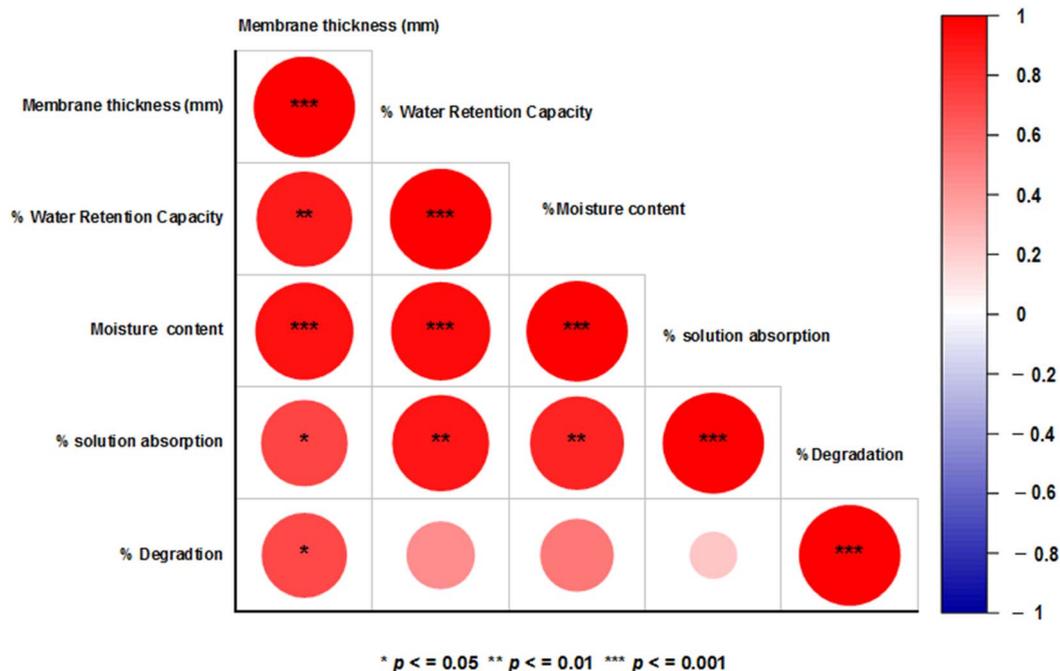**Fig. 15** Graphical representation of hemolytic activity of hydrogels.

Fig. 16 Correlation analysis of hydrogel membranes thickness, % water retention capacity, % moisture content, % solution absorption capacity, and % degradation.

creation of certain interactions of red blood cells with active groups of honey, aloe vera gel and citric acid. However, all hydrogel samples showed significantly less hemolytic/cytotoxicity activity than the positive control, which displayed nearly 100% hemolysis. Overall, these hydrogels' low hemolytic activity indicated that they can be used safely in wound healing applications.[64]

Fig. 16 correlation matrix illustrates the connections between hydrogel membranes thickness, % water retention capacity, % moisture content, % solution absorption capacity and % degradation. The size and color of the circles represent the strength and direction of the correlations, while the stars indicate their statistical significance. Hydrogel membrane thickness is strongly and positively correlated with % water retention capacity and moisture content, indicating that thicker hydrogel membranes are better at retaining water and maintaining moisture. Moisture content is also strongly positively correlated with % solution absorption capacity, showing that hydrogel membranes with higher moisture content absorb more solution. In contrast, % degradation is negatively correlated with properties like moisture content, % solution absorption capacity, and hydrogel membrane thickness, suggesting that hydrogel membranes with higher moisture or absorption capacity degrade less over time. % Water retention capacity also negatively correlates with % degradation, though the relationship is weaker. Notably, moisture content and % water retention capacity are highly interdependent, reinforcing their role in improving hydrogel functionality. Overall, the results suggested that thicker hydrogel membranes with high water retention, moisture content, and absorption capacity are more stable and less prone to degradation. This highlights the

importance of these properties in designing durable and effective hydrogel membranes.

3.9 Conclusion

This work presents a sustainable multifunctional hydrogel for wound care treatment, synthesized by the combination of chitosan/PVA with citric acid for crosslinking, and incorporating honey and aloe vera gel as bioactive agents. The process of freeze-gelation followed by CA crosslinking resulted in stable, highly porous structures with sponge-like microstructures as observed by SEM. Reduced O–H/N–H/amide band intensities in FTIR confirmed effective crosslinking, and an increase in amorphous character was observed by XRD. The CA-crosslinked formulation rich in honey and aloe vera (GG-08) exhibited the highest water-retention capacity (218%) and moisture content (99%). In contrast, the uncrosslinked GG-04 showed the most significant biodegradation ($93 \pm 3\%$), illustrating a balance between long-term stability and absorption. The hydrogels demonstrated broad-spectrum antibacterial activity with varying selectivity based on their composition. In addition, the hydrogels were particularly effective against *Staphylococcus aureus*, while CA-crosslinked GG-05 showed superior performance against *Escherichia coli* and *Klebsiella pneumoniae*. Anti-hemolysis tests confirmed low cytotoxicity across all formulations ($\leq{\sim}11\%$ hemolysis), indicating good hemocompatibility. Overall, CA-crosslinked chitosan/PVA hydrogels loaded with honey and Aloe vera meet essential criteria for superior wound dressings, including moisture balance, exudate management, antibacterial protection, and biocompatibility and offer an environmentally friendly alternative that uses toxic crosslinkers

such as glutaraldehyde. While the *in vitro* results are promising, future studies should focus on the study of covalent cross-linking and network density. Finally, the controlled release of bioactive compounds and their effectiveness against biofilms and multidrug-resistant pathogens should be assessed along with the validation for safety and efficacy *in vivo* to broaden the scope of developed hydrogels.

Conflicts of interest

There are not conflicts to declare.

Data availability

The data that support the findings of this study are available from the corresponding authors upon reasonable request.

Supplementary information is available. See DOI: https://doi.org/10.1039/d5ra05550d.

References

1 M. Zubair, S. Hussain, A. Hussain, M. E. Akram, S. Shahzad, Z. Rauf, M. Mujahid and A. Ullah, *Biomater. Sci.*, 2025, **13**, 130–160.

2 X. Liang, C. Huang, H. Liu, H. Chen, J. Shou, H. Cheng and G. Liu, *Chin. Chem. Lett.*, 2024, **35**, 109442.

3 J. Zhu, H. Cheng, Z. Zhang, K. Chen, Q. Zhang, C. Zhang, W. Gao and Y. Zheng, *Gels*, 2024, **10**, 495.

4 L. Yang, J. Li, L. Yang, W. Wang, Z. Yue, J. Li, L. Shi and T. Sun, *Appl. Organomet. Chem.*, 2024, **38**, e7328.

5 Y. Liang, J. He, M. Li, Z. Li, J. Wang, J. Li and B. Guo, *ACS Biomater. Sci. Eng.*, 2025, **11**, 1921–1944.

6 J. Duarte, F. Mascarenhas-Melo, P. C. Pires, F. Veiga and A. C. Paiva-Santos, *Eur. Polym. J.*, 2024, 113026.

7 A.-E. Segneanu, L. E. Bejenaru, C. Bejenaru, A. Blendea, G. D. Mogoşanu, A. Biţă and E. R. Boia, *Polymers*, 2025, **17**, 2026.

8 X. Zhang, Y. Wang, Z. Gao, X. Mao, J. Cheng, L. Huang and J. Tang, *J. Appl. Polym. Sci.*, 2024, **141**, e54746.

9 A. Sadeghianmaryan, N. Ahmadian, S. Wheatley, H. A. Sardroud, S. A. S. Nasrollah, E. Naseri and A. Ahmadi, *Int. J. Biol. Macromol.*, 2024, 131207.

10 M. Zubair, M. Mujahid, S. Shahzad, Z. Rauf, A. Hussain, M. Ayyash and A. Ullah, *Int. J. Biol. Macromol.*, 2025, 146070.

11 X. Zhang, Y. Liang, S. Huang and B. Guo, *Adv. Colloid Interface Sci.*, 2024, 103267.

12 S. Kaushik, Z. W. Ong, Y. K. Liew, W. M. Lim, L. C. Wong and Y. Y. Then, *J. Appl. Polym. Sci.*, 2025, e57827.

13 F. Amir, M. B. K. Niazi, U. S. Malik, Z. Jahan, S. Andleeb, T. Ahmad and Z. Mustansar, *Int. J. Biol. Macromol.*, 2024, **258**, 128831.

14 S. Shahzad and M. Mujahid, in *Green Biopolymers for Packaging Applications*, CRC Press, 2025, pp. 45–77.

15 P. Ding, X. Ding, J. Li, W. Guo, O. V. Okoro, M. Mirzaei, Y. Sun, G. Jiang, A. Shavandi and L. Nie, *Biomed. Mater.*, 2024, **19**, 025021.

16 M. T. Elabbasy, M. A. Samak, A. A. Saleh, E. S. El-Shetry, A. Almalki, M. El-Morsy and A. Menazea, *Mater. Chem. Phys.*, 2024, **328**, 129972.

17 S. Shahzad and M. Mujahid, in *Green Biopolymers for Packaging Applications*, CRC Press, pp. , pp. 45–77.

18 Y. Tang, L. Chen and X. Ran, *Nutrients*, 2024, **16**, 2455.

19 S. W. Chin, A. S. Azman and J. W. Tan, *Health Sci. Rep.*, 2024, **7**, e2251.

20 A. Kheradvar Kolour, S. Ghoraishizadeh, M. S. Zaman, A. Alemzade, M. Banavand, J. Esmaeili and M. Shahrousvand, *ACS Appl. Bio Mater.*, 2024, **7**(12), 8642–8655.

21 F. Rahmania and A. Fawzy, *Int. J. Med. Sci.*, 2024, **4**, 812–817.

22 A. Naskar, K. Chatterjee, K. Roy, A. Majie, A. B. Nair, P. Shinu, M. A. Morsy, N. Jain, M. Pandey and B. Gorain, *J. Pharmacol. Pharmacother.*, 2024, **15**, 5–18.

23 A. J. Khamene, F. Yazdian, M. Pourmadadi, M. Ghobeh, K. Khoshmaram, S. Fathi-karkan, A. Rahdar and S. Pandey, *Inorg. Chem. Commun.*, 2024, **168**, 112879.

24 M. C. Ceballos-Santa, A. Sierra, I. M. Zalbidea, E. Lazarus, V. Marin-Montealegre, S. Ramesh, P. Iglesias, K. Wuertz-Kozak and I. V. Rivero, *J. Biomed. Mater. Res. B Appl. Biomater.*, 2024, **112**, e35379.

25 D. N. A. Muslim, F. B. M. Said and N. Nambiar, *Int. J. Adv. Life sci. Res.*, 2024, **7**, 12–20.

26 H. Hamedi, S. Moradi, S. M. Hudson and A. E. Tonelli, *Carbohydr. Polym.*, 2018, **199**, 445–460.

27 C.-C. Kuo, H. Qin, Y. Cheng, X. Jiang and X. Shi, *Food Hydrocoll.*, 2021, **111**, 106262.

28 Q. Li, X. Lai, Y. Duan, F. Jiang, Y. Li, Z. Huang, S. Liu, Y. Wang, C. Jiang and C. Zhang, *Carbohydr. Polym.*, 2025, **348**, 122827.

29 P. L. Savekar, S. J. Nadaf, S. G. Killedar, V. M. Kumbar, J. H. Hoskeri, D. A. Bhagwat and S. S. Gurav, *Int. J. Biol. Macromol.*, 2024, **274**, 133366.

30 D. Simões, S. P. Miguel, M. P. Ribeiro, P. Coutinho, A. G. Mendonça and I. J. Correia, *Eur. J. Pharm. Biopharm.*, 2018, **127**, 130–141.

31 F. Islam, E. Rahman, T. Tarannum and N. Islam, *Compos., Part C: Open Access*, 2024, **15**, 100528.

32 A. Chhatri, J. Bajpai, A. Bajpai, S. Sandhu, N. Jain and J. Biswas, *Carbohydr. Polym.*, 2011, **83**, 876–882.

33 T. Shahzadi, M. Zaib, T. Riaz, S. Shehzadi, M. A. Abbasi and M. Shahid, *Arabian J. Sci. Eng.*, 2019, **44**, 6435–6444.

34 M. Mir and L. D. Wilson, *ACS Appl. Bio Mater.*, 2024, **7**(11), 7391–7403.

35 M. Mujahid, M. Zubair, A. Yaqoob, S. Shahzad and A. Ullah, *Bioengineering*, 2025, **12**, 439.

36 A. Kumar, T. Behl and S. Chadha, *Int. J. Biol. Macromol.*, 2020, **149**, 1262–1274.

37 N. Annabi, J. W. Nichol, X. Zhong, C. Ji, S. Koshy, A. Khademhosseini and F. Dehghani, *Tissue Engineering Part B: Reviews*, 2010, **16**, 371–383.

38 K. Shalumon, K. Anulekha, C. Girish, R. Prasanth, S. Nair and R. Jayakumar, *Carbohydr. Polym.*, 2010, **80**, 413–419.

39 S. Noori, M. Kokabi and Z. Hassan, *J. Appl. Polym. Sci.*, 2018, **135**, 46311.

© 2025 The Author(s). Published by the Royal Society of Chemistry

40 Y. Bai, Y. Niu, S. Qin and G. Ma, *Pharmaceutics*, 2023, **15**, 1913.

41 A. A. Maan, Z. F. R. Ahmed, M. K. I. Khan, A. Riaz and A. Nazir, *Trends Food Sci. Technol.*, 2021, **116**, 329–341.

42 A. Chang, Z. Ye, Z. Ye, J. Deng, J. Lin, C. Wu and H. Zhu, *Carbohydr. Polym.*, 2022, **291**, 119520.

43 R. Shi, J. Bi, Z. Zhang, A. Zhu, D. Chen, X. Zhou, L. Zhang and W. Tian, *Carbohydr. Polym.*, 2008, **74**, 763–770.

44 N. Shamsuri, S. Majid, M. Hamsan, S. Halim, N. Manan, M. Sulaiman, A. Jahidin, N. Halim, S. Aziz and M. Kadir, *J. Appl. Polym. Sci.*, 2024, **141**, e55303.

45 C. Chapa and Instituto de Ingeniería y Tecnología, *Rev. Mexic. Ingen. Biomed.*, 2023, **44**, 24–36.

46 A. Das, T. Ringu, S. Ghosh and N. Pramanik, *Polym. Bull.*, 2023, **80**, 7247–7312.

47 M. M. Mahamoud, T. M. Ketema, Y. Kuwahara and M. Takafuji, *Gels*, 2024, **10**, 527.

48 G. Biscari, 2023.

49 C. Wiegand, J. Tittelbach, U.-C. Hipler and P. Elsner, *Chronic Wound Care Management and Research*, 2015, 101–111.

50 S. V. Pochampally, J. G. Blanco, K. Ayalew, S. E. H. Murph and J. Moon, *Sep. Purif. Technol.*, 2024, **350**, 127793.

51 M. Zubair, S. Hussain, A. Hussain, M. E. Akram, S. Shahzad, Z. Rauf, M. Mujahid and A. Ullah, *Biomater. Sci.*, 2025, **13**, 130–160.

52 Y. Liang, J. He and B. Guo, *ACS Nano*, 2021, **15**, 12687–12722.

53 R. Salihu, S. I. Abd Razak, N. A. Zawawi, M. R. A. Kadir, N. I. Ismail, N. Jusoh, M. R. Mohamad and N. H. M. Nayan, *Eur. Polym. J.*, 2021, **146**, 110271.

54 N. E. F. Esa, M. N. M. Ansari, S. I. A. Razak, N. I. Ismail, N. Jusoh, N. A. Zawawi, M. I. Jamaludin, S. Sagadevan and N. H. M. Nayan, *Molecules*, 2022, **27**, 3080.

55 G. Yang, Z. Xiao, H. Long, K. Ma, J. Zhang, X. Ren and J. Zhang, *Sci. Rep.*, 2018, **8**, 1616.

56 S. Zhang, C. Liu, M. Su, D. Zhou, Z. Tao, S. Wu, L. Xiao and Y. Li, *J. Mater. Chem. B*, 2024, **12**, 11611–11635.

57 C. Ardean, C. M. Davidescu, N. S. Nemeş, A. Negrea, M. Ciopec, N. Duteanu, P. Negrea, D. Duda-Seiman and V. Musta, *Int. J. Mol. Sci.*, 2021, **22**, 7449.

58 B. Farasati Far, M. R. Naimi-Jamal, M. Sedaghat, A. Hoseini, N. Mohammadi and M. Bodaghi, *J. Funct. Biomater.*, 2023, **14**, 115.

59 D. K. Patel, E. Jung, S. Priya, S.-Y. Won and S. S. Han, *Carbohydr. Polym.*, 2024, **323**, 121408.

60 A. Mukhopadhyay, M. Rajput, A. Barui, S. S. Chatterjee, N. K. Pal, J. Chatterjee and R. Mukherjee, *Mater. Sci. Eng. C*, 2020, **116**, 111218.

61 M. Dada and P. Popoola, *Discov. Mater.*, 2024, **4**, 10.

62 S. Toufanian, Macroporous Hydrogels for Tissue Engineering and Wound Care, PhD thesis, 2023, **http://hdl.handle.net/11375/28497**.

63 Y. Zhang, J. Lu, T. Chang, X. Tang, Q. Wang, D. Pan, J. Wang, H. Nan, L. Liu and B. Qi, *J. Ethnopharmacol.*, 2023, 117409.

64 T. Zhao, N. Wang, Y. Wang, J. Yang, Y. Tang, Y. Wang, H. Wei, J. Yang, T. Yu and X. Sun, *Int. J. Biol. Macromol.*, 2024, 135724.